Identification of intracellular carriers for the endocannabinoid anandamide

Martin Kaczocha[a], Sherrye T. Glaser[b], and Dale G. Deutsch[a,1]

Departments of [a]Biochemistry and Cell Biology and [b]Neurobiology and Behavior, Stony Brook University, Stony Brook, NY 11794

Communicated by William J. Lennarz, Stony Brook University, Stony Brook, NY, February 10, 2009 (received for review December 22, 2008)

The endocannabinoid anandamide (arachidonoyl ethanolamide, AEA) is an uncharged neuromodulatory lipid that, similar to many neurotransmitters, is inactivated through its cellular uptake and subsequent catabolism. AEA is hydrolyzed by fatty acid amide hydrolase (FAAH), an enzyme localized on the endoplasmic reticulum. In contrast to most neuromodulators, the hydrophilic cytosol poses a diffusional barrier for the efficient delivery of AEA to its site of catabolism. Therefore, AEA likely traverses the cytosol with the assistance of an intracellular carrier that increases its solubility and rate of diffusion. To study this process, AEA uptake and hydrolysis were examined in COS-7 cells expressing FAAH restricted to the endoplasmic reticulum, mitochondria, or the Golgi apparatus. AEA hydrolysis was detectable at the earliest measurable time point (3 seconds), suggesting that COS-7 cells, normally devoid of an endocannabinoid system, possess an efficient cytosolic trafficking mechanism for AEA. Three fatty acid binding proteins (FABPs) known to be expressed in brain were examined as possible intracellular AEA carriers. AEA uptake and hydrolysis were significantly potentiated in N18TG2 neuroblastoma cells after overexpression of FABP5 or FABP7, but not FABP3. Similar results were observed in COS-7 cells stably expressing FAAH. Consistent with the roles of FABP as AEA carriers, administration of the competitive FABP ligand oleic acid or the selective non-lipid FABP inhibitor BMS309403 attenuated AEA uptake and hydrolysis by ≈50% in N18TG2 and COS-7 cells. Taken together, FABPs represent the first proteins known to transport AEA from the plasma membrane to FAAH for inactivation and may therefore be novel pharmacological targets.

fatty acid amide hydrolase | fatty acid binding protein | transport

The endocannabinoid anandamide (arachidonoyl ethanolamide, [AEA]) is a neuromodulatory lipid that belongs to a family of signaling molecules collectively termed endocannabinoids (1). The biological actions of AEA are tightly controlled through its enzymatic synthesis and degradation (2). Like Δ^9-tetrahydracannabinol, AEA activates the central and peripheral cannabinoid receptors CB_1 and CB_2 and is also a ligand for transient receptor potential vanilloid receptor 1 (3–7). Cannabinoid receptors mediate numerous physiological processes including analgesia, vasodilation, neuroprotection, cognitive functions, movement, and the regulation of food intake (8, 9).

Most neurotransmitters (e.g., catecholamines, glutamate, and serotonin) are hydrophilic molecules requiring protein transporters to traverse the plasma membrane. Once inside cells, they freely diffuse through the cytosol to their sites of catabolism. In contrast, AEA is an uncharged lipid capable of traversing the bilayer unaided (10). Accordingly, several studies concluded that AEA uptake occurs by passive diffusion (10–15), although facilitated diffusion and/or endocytosis have also been proposed (16–20).

Regardless of the uptake mechanism at the plasma membrane, the hydrophobic character of AEA is expected to limit its diffusion through the aqueous cytosol. Because AEA is hydrolyzed primarily by FAAH, an endoplasmic reticulum (ER)-localized enzyme (21, 22), it is likely that a chaperone mechanism rapidly delivers AEA from the plasma membrane to FAAH. To date, no intracellular carriers/chaperones have been identified for endocannabinoids. As AEA is efficiently metabolized by numerous cell types including FAAH-transfected cells normally devoid of a functional endocannabinoid system (23–25), a ubiquitous mechanism(s) to shuttle AEA must exist. Consequently, candidate intracellular AEA carriers are likely widely expressed and capable of binding a variety of lipophilic ligands. The FABP family of lipid carriers fits both of these criteria (26). These proteins are widely expressed in mammalian tissues, with three of its members, FABP3, FABP5, and FABP7, expressed in brain (26–32). In addition to fatty acids, these proteins carry other lipophilic ligands such as retinoic acid (33). Here, we present evidence that FABPs function as intracellular carriers for AEA.

Results

AEA Cellular Uptake Is Rapid and Independent of Subcellular Localization of FAAH. To explore putative trafficking mechanisms that may deliver AEA to intracellular FAAH, we designed FAAH variants with distinct subcellular localizations. The rationale for this is as follows: if AEA primarily uses a directional mechanism for internalization (e.g., endocytosis), then AEA would be preferentially delivered to a specific target intracellular organelle. However, if AEA trafficking to FAAH involves a carrier protein, its intracellular transport should be unaffected by the subcellular localization of FAAH.

COS-7 cells do not express FAAH and are therefore suitable for FAAH re-localization studies (34). Rat FAAH was fused to eGFP at its C terminus (Fig. 1*A*). The N-terminal transmembrane (TM) helix of FAAH (residues 1–29), which is dispensable for activity (35), was removed to allow the generation of other ΔTM-FAAH-eGFP fusion proteins. To localize FAAH to outer mitochondrial membranes or the Golgi apparatus, ΔTM-FAAH-eGFP was respectively fused at its N terminus to the mitochondrial outer membrane targeting sequence from TOM20 (36) or the Golgi resident protein Grasp65 (37).

Stable cell lines expressing these fusion proteins were generated and similar expression levels were confirmed by Western blotting and activity assays (Figs. 1*B* and 1*C*). Wild-type FAAH-eGFP (COS7-FAAH-eGFP) localized to the ER in agreement with a previous study (38). TOM-ΔTMFAAH-eGFP and GRASP-ΔTMFAAH-eGFP were confined to the mitochondria and Golgi apparatus, respectively (Fig. 1*D*). Protease protection experiments confirmed that all FAAH variants occupied the cytoplasmic face of membranes (Fig. 1*E*). Therefore, the cytosol represents the sole barrier for AEA delivery from the plasma membrane to FAAH.

AEA uptake and hydrolysis assays determined whether relocalization of FAAH to these organelles affected AEA inactivation. These assays tracked the cellular uptake of [^{14}C]AEA and its subsequent breakdown into [^{14}C]ethanolamine by FAAH (12). AEA uptake is coupled to its hydrolysis by FAAH, which maintains

Author contributions: M.K., S.T.G., and D.G.D. designed research; M.K. and S.T.G. performed research; M.K. and D.G.D. analyzed data; and M.K., S.T.G., and D.G.D. wrote the paper.

The authors declare no conflict of interest.

[1]To whom correspondence should be addressed at: Department of Biochemistry and Cell Biology, Stony Brook University, Stony Brook, NY 11794-5215. E-mail: ddeutsch@notes.sunysb.edu.

This article contains supporting information online at www.pnas.org/cgi/content/full/0901515106/DCSupplemental.

NEUROSCIENCE

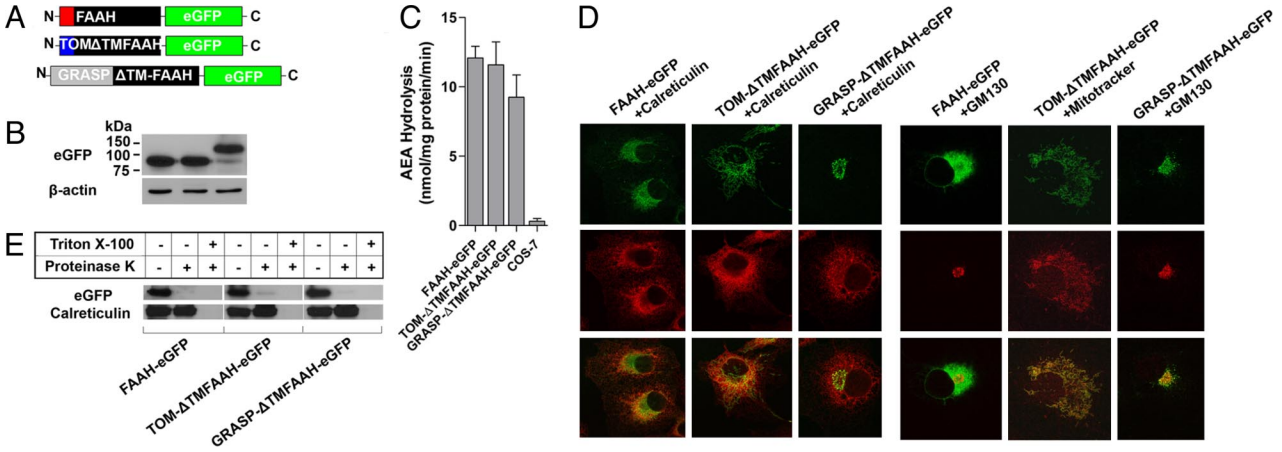

Fig. 1. Generation of FAAH variants with distinct subcellular localizations. (*A*) Constructs used in this study. FAAH-eGFP is shown with its N-terminal transmembrane helix (residues 1–29) in red, residues 30–579 in black, and eGFP in green. In TOM-ΔTMFAAH-eGFP, the N-terminal helix was replaced with the N terminus of mouse TOM20 (blue, residues 1–33). In GRASP-ΔTMFAAH-eGFP, the Golgi resident protein grasp65 (gray) was fused to the N terminus of ΔTMFAAH-eGFP. (*B*) Western blot indicates similar protein levels in homogenates of COS-7 cells stably expressing FAAH-eGFP, TOM-ΔTMFAAH-eGFP, or GRASP-ΔTMFAAH-eGFP. Blots were probed with eGFP antibodies with β-actin serving as a loading control. (*C*) Similar rates of [^{14}C]AEA hydrolysis (100 μM) were observed in COS7-FAAH-eGFP, TOM-ΔTMFAAH-eGFP, and GRASP-ΔTMFAAH-eGFP homogenates ($n = 3$). (*D*) FAAH fusion protein localization is restricted to specific organelles. *Top panel* shows FAAH-eGFP fusion proteins (green); *middle panel* depicts the marker of interest (red); and *bottom panel* is the merged image (yellow). FAAH-eGFP localized to the ER and mostly overlapped with the ER marker, calreticulin. TOM-ΔTMFAAH-eGFP co-localized with the mitochondrial dye Mitotracker CM-H2Xros and was excluded from the ER. As confirmed by double labeling with GM130, GRASP-ΔTMFAAH-eGFP localized to the Golgi apparatus in COS-7 cells. Note that overexpression of GRASP-ΔTMFAAH-eGFP resulted in an enlargement of the Golgi apparatus. (*E*) Proteinase K protection analysis of FAAH-eGFP, TOM-ΔTMFAAH-eGFP and GRASP-ΔTMFAAH-eGFP proteins in membrane fractions of COS-7 cells. Membranes were either left untreated or were incubated with 500 μg/ml proteinase K in the presence or absence of 1% Triton X-100. Samples were subsequently resolved by SDS/PAGE and probed with eGFP and calreticulin antibodies.

an outward/inward concentration gradient that increases AEA accumulation in the steady state (12, 39, 40). Therefore, if AEA delivery to FAAH is reduced when FAAH expression is confined to the Golgi apparatus or mitochondria, the reduced hydrolysis of AEA will lower the AEA gradient and diminish its uptake. Conversely, enhanced AEA delivery to FAAH will result in increased hydrolysis of AEA and elevated accumulation.

The uptake and hydrolysis of [^{14}C]AEA was similar between COS7-FAAH-eGFP, TOM-ΔTMFAAH-eGFP, and GRASP-ΔTMFAAH-eGFP cells at 5 minutes (Fig. 2*A*). As this time point may allow for AEA to be taken up through one mechanism and subsequently redistributed intracellularly by others, these experiments were repeated using shorter time points. Similar to the results at 5 minutes, [^{14}C]AEA uptake and hydrolysis were unchanged between the three cell lines at 10 seconds (Fig. 2*B*). Identical results were obtained when the intracellular hydrolysis of [^{14}C]AEA after uptake was examined at 3 seconds, with hydrolysis being similar in cells expressing all FAAH variants and significantly lower in cells lacking FAAH (Fig. 2*C*). These data suggest that AEA uptake and its subsequent delivery from the plasma membrane to FAAH occurs through an extremely rapid and organelle non-selective mechanism.

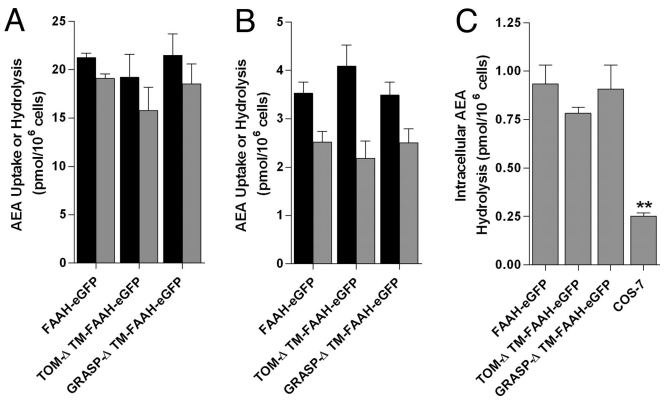

Fig. 2. Rapid inactivation of AEA in cells expressing spatially restricted FAAH variants. [^{14}C]AEA (100 nM) uptake (black bars) and hydrolysis (gray bars) were similar ($P > 0.05$) in COS7-FAAH-eGFP, TOM-ΔTMFAAH-eGFP, or GRASP-ΔTMFAAH-eGFP cells after (*A*) 5-minute or (*B*) 10-second incubations ($n = 3$). (*C*) Similar levels of intracellular [^{14}C]AEA hydrolysis after 3-second incubation in COS7-FAAH-eGFP, TOM-ΔTMFAAH-eGFP, or GRASP-ΔTMFAAH-eGFP cells ($P > 0.05$). Hydrolysis of [^{14}C]AEA in untransfected COS-7 cells was significantly lower than in FAAH-eGFP expressing controls. **, $P < 0.01$ ($n = 3$).

Uptake and Subsequent Hydrolysis of AEA Are Enhanced by FABP5 and FABP7. The results presented thus far suggest that the transmembrane transport and subsequent intracellular delivery of AEA to FAAH is rapid. The hydrophobicity of AEA (estimated LogP value of 5.1 (41)) suggests that it is unlikely to diffuse efficiently from the plasma membrane to intracellular membranes containing FAAH unaided. Because AEA is taken up and hydrolyzed by all cells that natively express and those transfected with FAAH (23–25), it is likely that AEA may share an intracellular delivery system used by other endogenous lipophilic molecules. Therefore, we focused upon the well-characterized class of fatty acid carriers, the FABPs. Three members of the FABP family are expressed in brain, FABP3, FABP5, and FABP7 (26). To determine whether these FABPs can potentiate AEA uptake and hydrolysis, COS7-FAAH-eGFP cells were transfected with each FABP and AEA uptake and metabolism analyzed. Following a 10-minute incubation in uptake media, overexpression of FABP5 and FABP7 but not FABP3 significantly enhanced [^{14}C]AEA uptake by 32% and 35%, respectively (Fig. 3*A*). AEA hydrolysis was proportionally and significantly elevated. Similar effects, albeit slightly lower in magnitude, were observed after a shorter incubation time of 5 minutes (data not shown). Western blotting confirmed that all three FABPs were successfully expressed in COS-7 cells (Fig. 3*B*). The hydrolysis of [^{14}C]AEA was similar in homogenates of vector transfected cells and in cells transfected with the FABPs (Fig. 3*C*), confirming that the overexpression of FABPs did not artifactually influence AEA uptake by modulating FAAH expression and/or activity.

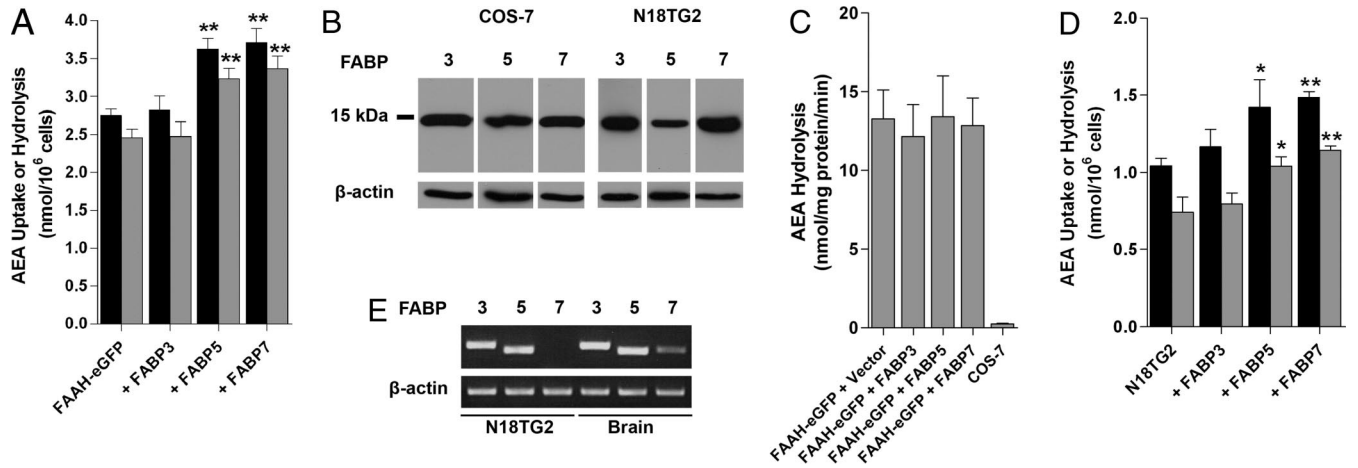

Fig. 3. Effect of FABP overexpression upon AEA uptake and hydrolysis. (*A*) Following a 10-minute incubation, [^{14}C]AEA uptake (black bars) and hydrolysis (gray bars) were elevated in COS-7-FAAH-eGFP cells after FABP5 or FABP7, but not FABP3, transfection. **, $P < 0.01$ compared with vector-transfected controls ($n = 3$–5). (*B*) Western blot confirms the overexpression of FABP3, FABP5, or FABP7 in COS-7-FAAH-eGFP- and N18TG2-transfected cells. (*C*) Overexpression of FABP3, FABP5, or FABP7 had no effect upon [^{14}C]AEA hydrolysis by COS-7-FAAH-eGFP homogenates ($P > 0.05$). (*D*) [^{14}C]AEA uptake and hydrolysis by N18TG2 cells are enhanced after transfection with FABP5 and FABP7, but not FABP3. *, $P < 0.05$ and **, $P < 0.01$ compared with vector transfected controls ($n = 3$–5). (*E*) RT-PCR analysis confirmed the endogenous expression of FABP3, FABP5, and FABP7 in brain and the expression of FABP3 and FABP5 in N18TG2 cells. β-Actin serves as a control.

To confirm that the function of FABPs as AEA carriers is independent of cell type, these experiments were repeated in mouse neuroblastoma N18TG2 cells. These cells express CB_1 receptors, FAAH, and can take up and hydrolyze AEA (11, 42, 43). Similar to the results in COS-7 cells, overexpression of FABP5 and FABP7 significantly enhanced the uptake of [^{14}C]AEA by 36% and 42%, respectively (Fig. 3*D*). AEA hydrolysis was also proportionally and significantly elevated. Similar to COS-7 cells, Western blotting confirmed that N18TG2 cells transfected with FABPs overexpressed these proteins (Fig. 3*B*). To confirm that these proteins constitute the endogenous repertoire of FABPs in N18TG2 cells, we performed RT-PCR analysis in N18TG2 cells and mouse brain as a control. As expected, and in accordance with previous data (44, 45), FABP3, FABP5, and FABP7 were expressed in brain (Fig. 3*E*). Similarly, N18TG2 cells expressed FABP3 and FABP5, but not FABP7 (Fig. 3*E*). The lack of FABP7 expression in N18TG2 cells is consistent with the observation that FABP7 expression is confined to glial cells in the brain (46). Collectively, these data suggest that FABPs function as intracellular carriers for AEA.

Inhibition of FABPs Reduces AEA Uptake and Hydrolysis. We used competitive FABP ligands/inhibitors to examine the role of endogenous FABPs in cytosolic trafficking of AEA to FAAH. COS7-FAAH-eGFP and N18TG2 cells were incubated with the FABP ligand oleic acid (100 μM) (47) and [^{14}C]AEA uptake measured after a 5-minute incubation. Oleic acid reduced the uptake of [^{14}C]AEA in COS7-FAAH-eGFP and in N18TG2 cells by 25 and 53%, respectively (Fig. 4*A*). Because oleic acid lacks selectivity for FABPs, we repeated these studies using the novel FABP inhibitor BMS309403 (48). BMS309403 is a competitive inhibitor of FABPs with reported IC_{50} values of 250 and 350 nM for FABP3 and FABP5, respectively (26, 48). Treatment of COS7-FAAH-eGFP or N18TG2 cells with 20–100 μM BMS309403 resulted in a dose-dependent reduction in [^{14}C]AEA uptake with a maximal inhibition of 48% and 57%, respectively (Figs. 4*B* and 4*C*). AEA hydrolysis was proportionally and significantly reduced. Remarkably, BMS309403 also reduced the intracellular hydrolysis of [^{14}C]AEA after uptake at 3 seconds in both cell types (Figs. 4*D* and 4*E*) without affecting the levels of cell associated [^{14}C]AEA (data not shown). This confirms that BMS309403 potently attenuates the rapid intracellular trafficking of AEA to FAAH but not its delivery from the media to cells. The potency of BMS309403 was preserved in cells that were pretreated with this inhibitor but subsequently incubated with [^{14}C]AEA alone (data not shown), confirming that its ability to reduce AEA uptake stems from the inhibition of a cellular target(s) rather than from artifactual competition for BSA binding in the incubation media. BMS309403 and oleic acid did not inhibit FAAH activity over the concentration range used in this study [supporting information (SI) Fig. S1], suggesting that their effects upon [^{14}C]AEA uptake and metabolism result from inhibition of intracellular transport rather than FAAH.

Discussion

The transient nature of lipid neurotransmitter signaling requires both efficient synthetic enzymes and a mechanism(s) for rapid ligand clearance and inactivation. The presence of cannabinoid receptors on the plasma membrane and FAAH on the ER ensures that sites of AEA signaling are physically separated from its primary site of catabolism. The low solubility of AEA in the hydrophilic cytosol likely poses a diffusional barrier and suggests that intracellular proteins may facilitate its trafficking from the plasma membrane to FAAH (40, 49).

Similar to AEA, the cytoplasm also presents an energetically unfavorable barrier to the diffusion of fatty acids. To obviate this, intracellular proteins such as FABPs orchestrate the movement of free fatty acids inside cells (26, 50). FABPs are widely expressed in the central nervous system and the periphery (26–32) and may therefore serve as intracellular carriers for AEA in various tissues. In the brain, FABP3 and FABP5 are expressed in neurons while FABP7 is primarily localized in glial cells (27, 46, 51). The wide distribution of FABPs in the mammalian brain (27, 31) suggests that these proteins may coordinate the delivery of AEA to FAAH throughout the brain.

Our finding that AEA is rapidly and efficiently delivered to FAAH regardless of the enzyme's subcellular localization is consistent with a trafficking mechanism using cytosolic carrier proteins such as FABPs. FABPs may also provide a means for rapid substrate delivery to other enzymes with distinct subcellular localizations capable of metabolizing AEA to a minor degree (34, 52, 53). Relative to other AEA uptake models, the proposed mechanism of simple diffusion across the plasma membrane and subsequent cytosolic trafficking by FABPs provides the most temporally efficient mode of AEA delivery to FAAH. It is expected to be more efficient than the free diffusion of AEA across the cytosol or the

NEUROSCIENCE

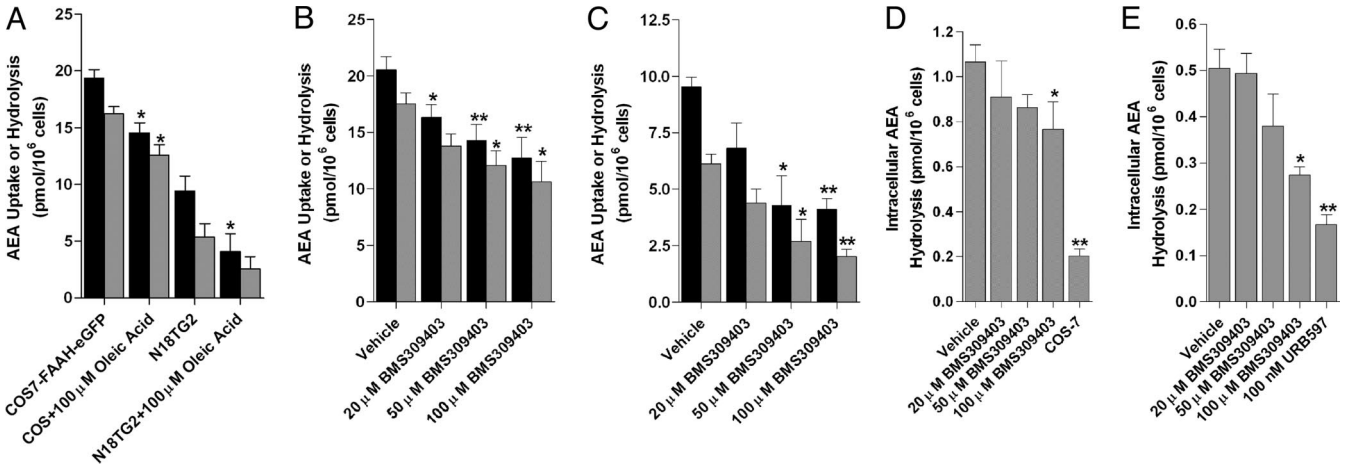

Fig. 4. Effect of FABP inhibition upon AEA internalization and hydrolysis by FAAH. (*A*) Treatment of COS-7-FAAH-eGFP and N18TG2 cells for 5 minutes with 100 μM oleic acid, a ligand for FABPs, significantly reduced [^{14}C]AEA uptake (black bars) and hydrolysis (gray bars). *, $P < 0.05$ compared with vehicle-treated controls ($n = 3$–5). (*B, C*) Treatment with 20–100 μM BMS309403, a selective competitive FABP inhibitor, significantly decreased [^{14}C]AEA uptake and metabolism by COS-7-FAAH-eGFP (*B*) or N18TG2 (c) cells at 5 min. *, $P < 0.05$ and **, $P < 0.01$ compared with vehicle controls ($n = 3$–5). (*D*, *E*) Increasing concentrations (20–100 μM) of BMS309403 reduced the hydrolysis of [^{14}C]AEA after cellular uptake by COS7-FAAH-eGFP (*D*) or N18TG2 (*E*) cells at 3 sec. *, $P < 0.05$ and **, $P < 0.01$ compared with vehicle-treated controls ($n = 3$–5).

movement of endocytic vesicles. For example, cytosolic free diffusion of AEA is expected to be a relatively slow process, as the structurally related stearate requires up to 200 seconds to diffuse half-way across the cytosol of a 20-μm hepatic cell (54, 55).

The contribution of FABPs as AEA carriers was revealed by overexpression and inhibition studies. Transfected FABP5 and FABP7 significantly enhanced AEA uptake and hydrolysis beyond the capacity of the endogenous FABP pool, suggesting that these proteins bind AEA with higher affinity than FABP3. These data are consistent with a recent report demonstrating that AEA binds FABP7 with a three-fold higher affinity than FABP3 (IC_{50} values of 5 vs. 15 μM, respectively), as judged by displacement of a fluorescent probe (56). Similar displacement values were observed for arachidonic acid. Therefore, the potentiation of AEA uptake after FABP transfection likely reflects direct binding to FABPs. Although FABP3 may not act as a high affinity carrier for AEA, its wide distribution throughout the central nervous system and the periphery suggests it could function as an AEA carrier in an auxiliary capacity. Prior observations that cultured cells accumulate intracellular AEA at concentrations in excess of those found in the media (the "AEA sink") (25, 40, 57) may be caused by membrane binding with a possible contribution of FABPs or other intracellular binding proteins.

The importance of FABPs as binding proteins for AEA was further demonstrated through inhibition studies. We found that oleic acid, a ligand for FABPs (47), significantly reduced the uptake and hydrolysis of AEA. This effect is in agreement with a previous study that observed AEA uptake inhibition by arachidonic acid (57). These effects were replicated after treatment with BMS309403 (48), a novel reversible FABP inhibitor. This inhibitor has previously been shown to reduce stearate uptake by adipocytes in a concentration dependent manner (32), with uptake in the presence of 50 or 100 μM BMS309403 reduced by $\approx$30% and 40%, respectively. The reduction of AEA uptake in COS-7 and N18TG2 cells treated with BMS309403 somewhat mirrors the inhibition of stearate internalization in adipocytes treated with the same concentrations of BMS309403 (32), suggesting that the contributions of FABPs toward AEA uptake may be similar to those of certain fatty acids. Neither oleic acid nor BMS309403 completely blocked AEA internalization or hydrolysis reflecting incomplete FABP inhibition, binding to BSA or other cellular proteins, or other mechanisms for cytosolic transport (e.g., inhibitor-insensitive carriers and/or endocytosis).

The involvement of FABPs as intracellular AEA trafficking proteins may resolve several phenomena of AEA uptake and metabolism that have remained unexplained, such as the ubiquitous nature of AEA delivery to FAAH, even in cells devoid of an endocannabinoid system after transfection with FAAH. We hypothesize that the capability of many cell types to deliver AEA to transfected FAAH may coincide with the expression of FABPs.

Another unresolved phenomenon involves the hundreds of lipophilic pharmacological inhibitors of AEA internalization. Although many of these structural analogs of AEA reduce its uptake by inhibiting FAAH (11, 12, 58, 59), several compounds have recently been described that do not appreciably inhibit this enzyme (60, 61). Several groups have hypothesized these compounds may act upon a putative AEA membrane transporter; however, it has also been speculated that these compounds inhibit intracellular trafficking proteins (11, 12, 14, 23). We propose that these inhibitors compete with AEA for binding to commonly expressed intracellular carriers such as FABPs. For example, the inhibitor AM1172 reduced AEA accumulation in cultured neurons, whereas OMDM1 inhibited AEA uptake in HaCaT keratinocytes (38, 61). Accordingly, neurons express FABP3 and FABP5 while HaCaT cells express FABP5 (27, 33).

The role of FABPs as intracellular carriers may well extend beyond the endocannabinoid AEA. The structural similarity between AEA and related N-acylethanolamines (e.g., palmitoylethanolamide and oleoylethanolamide) suggests that FABPs may likewise mediate their intracellular delivery to inactivating enzymes such as FAAH. Such a mechanism may also be in place to traffic the endocannabinoid 2-arachidonoylglycerol (2-AG). FABPs may also shuttle these lipids to the nucleus, wherein they activate peroxisome proliferators-activated receptors (PPARs) (62, 63). Such a function has been proposed for FABPs (56). This hypothesis is supported by a recent report that FABP5 mediates the nuclear translocation of retinoic acid and enhances its activation of nuclear PPARs (33).

From a health-related viewpoint, understanding the mechanism(s) of endocannabinoid inactivation may lead to new treatments for a variety of disorders, including addiction, pain, inflammation, and appetite regulation (64–66). Similar to FAAH inhibitors, compounds that target FABPs may attenuate the clearance and inactivation of AEA in a tissue and cell-type–specific manner, thereby raising its levels at cannabinoid receptors and enhancing the endocannabinoid tone.

Methods

Chemicals. AEA, oleic acid, and URB597 ([3-(3-carbamoylphenyl)phenyl] N-cyclohexylcarbamate) were obtained from Cayman Chemical (Ann Arbor, MI). BMS309403 (2′-(5-ethyl-3,4-diphenyl-1H-pyrazol-1-yl)(1,1′-biphenyl)-3-yl)oxy)-acetic acid) was from Calbiochem (San Diego, CA). Fatty acid-free bovine serum albumin (BSA) and phenylmethylsulfonyl fluoride (PMSF) were from Sigma (St. Louis, MO). [^{14}C]AEA (arachidonoyl [1-^{14}C]ethanolamide, 53 mCi/mmol) was kindly provided by the Drug Supply Program at the National Institute on Drug Abuse.

Cell Culture and Generation of Stable Cell Lines. COS-7 and N18TG2 cells were grown in Dulbecco's modified Eagle's medium (DMEM) supplemented with 10% fetal bovine serum (FBS), 100U/ml penicillin/streptomycin, 2 mM L-glutamine, and 1 mM sodium pyruvate in a humidified incubator containing 95% air and 5% CO_2. Transfections were carried out using Lipofectamine 2000 (Invitrogen, Carlsbad, CA) according to the manufacturer's instructions. For stable cell selection, 48 hours after transfection cells were expanded in medium containing 750 μg/ml geneticin (Invitrogen, Carlsbad, CA). Four weeks later, stable cells were subjected to flow cytometry at the Flow Cytometry Core Facility in Stony Brook University, and cells expressing identical levels of the indicated FAAH-eGFP fusion proteins were collected and expanded.

Cloning of Spatially Restricted FAAH Variants and FABPs. Rat FAAH was polymerase chain reaction (PCR) amplified and subcloned into the eGFP-N1 plasmid (Clontech) using XhoI and KpnI and the following primers: forward 5′-TATA*CTCGAG***GCCACC**ATGGTGCTGAGCGAAGTGTG-3′ and reverse 5′-TATAT*GGTACC*GACGATGGCTGCTTTTGAGG-3′. Underlined nucleotides represent restriction sites, while those in boldface type represent a Kozak consensus sequence. ΔTM-FAAH was subcloned into eGFP-N1 using XhoI and KpnI and the following primers: forward 5′-TATAT*CTCGAG*CGATGGACCGGGCGCCAG-3′ and reverse 5′-GATATAT*GGTACC*GACGATGGCTGCTTTTGAGG-3′. To localize FAAH to mitochondrial outer membranes, TOM20 (residues 1–33) was fused to the N terminus of ΔTM-FAAH-eGFP using NheI and XhoI and the following primers: forward 5′-GATATA*GCTAGC***GCCACC**ATGGTGGGCCGGAACAGC-3′ and reverse 5′-GATATA*CTCGAG*GTTGGGGTCACTCCGCCTTT-3′. To localize FAAH to the Golgi apparatus, Grasp65 was fused to the N terminus of ΔTM-FAAH-eGFP using NheI and EcoRI. This ΔTM-FAAH-eGFP was fused to eGFP-N1 using EcoRI and KpnI rather than XhoI to facilitate subcloning of Grasp65. The following primers were used: forward 5′-GATATA*GCTAGC***GCCACC**ATGGGGCTAGGGGCAAGC-3′ and reverse 5′-GATATA*GAATTCC*AGCCCAGGCTCTGGATCTGG-3′. FABP3, FABP5, and FABP7 were cloned from mouse brain RNA using PCR and the following primers: FABP3 forward 5′-GATATA*AAGCTT***GCCACC**ATGGCGGACGCCTTTGTC-3′ and reverse 5′- GATATA*CTCGAG*TCACGCCTCCTTCTCATAAGTC-3′, FABP5 forward 5′- GATATA*AAGCTT***GCCACC**ATGGCCAGCCTTAAGGATC-3′ and reverse 5′-GATATA*CTCGAG*TCATTGCACCTTCTCATAGAC-3′, and FABP7 forward 5′-GATA*GGTACC***GCCACC**ATGGTAGATGCTTTCTGCGCAA-3′ and reverse 5′- GATATA*CTCGAG*CTATGCCTTTTCATAACAGCGAAC-3′. FABP3 and FABP5 were digested with HindIII and XhoI, and FABP7 was cut with XhoI and KpnI and inserted into pcDNA4. All constructs were verified by DNA sequencing.

Immunolocalization of Fusion Proteins. COS-7 cells stably expressing the indicated constructs were plated unto coverslips. To assess mitochondrial localization, the cells were treated with 175 nM Mitotracker Red CM-H_2XRos (Molecular Probes, Eugene, OR) in DMEM + 10% FBS for 25 minutes at 37 °C, followed by fixation in 3% paraformaldehyde. For ER and Golgi apparatus co-localization studies, cells were processed essentially as described (11). Briefly, after fixation, cells were permeabilized with 0.2% Triton X-100 at 4 °C for 5 minutes and treated with rabbit anti-calreticulin antibodies (1:200) (Affinity Bioreagents, Golden, CO) or mouse anti-GM130 antibodies (1:100) (BD Transduction Labs, San Jose, CA) in 5% normal goat serum followed by donkey anti-rabbit or donkey anti-mouse IgG Alexa Fluor 594 (1:800) (Molecular Probes, Eugene, OR). All images were acquired using a Zeiss LSM 510 META NLO Two-Photon Laser Scanning Microscope.

Western Blotting. Either 10 μm of protein (stable cell lines) or 50 μm of protein (FABP-transfected cells) were run on a 10% sodium dodecyl sulfate/polyacrylamide gel electrophoresis (SDS/PAGE) gel. After transfer to a nitrocellulose membrane at 100 V for 25 min, the blots were blocked for 1 hour in 5% nonfat dry milk in phosphate-buffered saline (PBS) Tween (PBST). The blots were probed with rabbit anti-eGFP (1:2000) (Molecular Probes, Eugene, OR), mouse anti-β actin (1:10000–1:100000) or mouse anti-FABP3 (1:100) (Abcam, Cambridge, MA), rabbit anti-FABP5 (1:100) or rabbit anti-FABP7 (1:100) (Santa Cruz Biotechnology, Santa Cruz, CA) antibodies for 1 hour with shaking. The blots were rinsed three times with PBST followed by incubation with goat anti-mouse or goat anti-rabbit IgG HRP-conjugated antibodies (Molecular Probes, Eugene, OR) for 1 hour. The blots were rinsed three times with PBST, developed using the Immun-star HRP substrate (Bio-Rad, Hercules, CA) and exposed to film.

Proteinase K Protection Analysis. COS-7 cells were homogenized by passage through a 26-gauge needle in buffer A (10 mM HEPES-NaOH pH 7.5 containing 1 mM EDTA, 1.5 mM $MgCl_2$, 10 mM KCl and 250 mM sucrose). Unbroken cells and nuclei were pelleted by centrifugation at 1000 *g* for 10 minutes and the resulting supernatant was subjected to centrifugation at 100,000 *g* for 60 minutes at 4 °C. The pellet containing membranes was resuspended in buffer B (50 mM Tris pH 8, 3 mM $CaCl_2$, 1.5 mM $MgCl_2$, 10 mM KCl, 100 mM NaCl, 250 mM sucrose) and treated with 500 μg/ml proteinase K for 30 minutes at 37 °C in the presence or absence of 1% Triton X-100, or left untreated. The reactions were quenched by the addition of 20 mM PMSF. Control experiments using Proteinase K pretreated with PMSF revealed near complete inhibition of the enzyme (data not shown). The samples were separated by SDS/PAGE and visualized by immunoblotting with anti-eGFP or anti-calreticulin (1:2000) (Affinity Bioreagents, Golden, CO) antibodies.

FAAH Enzyme Assays. FAAH activity assays were performed as previously described (12). Briefly, cell homogenates were incubated with 100 μM AEA + 0.1 μCi [^{14}C]AEA in Tris-HCl (pH 9) containing 0.1% BSA. For activity analysis, time and total protein were adjusted to maintain substrate conversion at ≈10%. For inhibitor studies, 50 μg of COS-7 or 100 μg N18TG2 homogenates were pretreated with 100 μM oleic acid, BMS309403, or vehicle (DMSO) control for 15 minutes followed by incubation with [^{14}C] AEA (100 μM) for 1 or 30 minutes, respectively. Reactions were stopped by the addition of two volumes of 1:1 chloroform:methanol and the phases separated by centrifugation. The methanol phase (containing [^{14}C]ethanolamine) was sampled and quantified using a Beckman LS 6500 scintillation counter.

Determination and Inhibition of AEA Cellular Uptake and Hydrolysis. The experiments were performed essentially as described (12). Cells were plated at ≈90% confluency in 35-mm dishes, washed twice in DMEM, and preincubated with the desired pharmacological compounds or vehicle controls (EtOH or DMSO). The cells were washed twice in DMEM and subsequently incubated for 5 minutes, 10 minutes, or 3 seconds, with 750 μl [^{14}C]AEA (100 nM) that was pre-equilibrated for 75 minutes in medium containing 0.15% BSA. The equilibration step is necessary to avoid uneven distribution of the radiotracer and to ensure that it is stable in solution prebound to BSA. Less than 1% of AEA was hydrolyzed during this preequilibration step (data not shown). Following the incubation, 750 μl of ice-cold DMEM + 0.15% BSA was added to the plates, the media separated from cells, which were then washed with DMEM + 0.15% BSA to remove nonspecifically bound AEA. The cells were scraped three times with 400 μl of ice-cold 2 mM ethylenediaminetetraacetic acid (EDTA) in PBS and chloroform:methanol (1:1) added to the media and cells and the phases separated by centrifugation. The resulting aqueous (containing [^{14}C]ethanolamine) and organic (containing intact [^{14}C]AEA) phases were counted by liquid scintillation counting. [^{14}C]AEA uptake was determined by summing the production of [^{14}C]ethanolamine in the media and cells with intact cellular [^{14}C]AEA. Hydrolysis of [^{14}C]AEA was quantified by production of [^{14}C]ethanolamine in the media and cells. Blanks consisting of either untransfected COS-7 cells or N18TG2 cells treated with 100 nM of the FAAH inhibitor URB597 were subtracted from all conditions.

Reverse Transcription–Polymerase Chain Reaction Analysis of Endogenous FABP Expression. A 1-μg quantity of RNA extracted from mouse brain or N18TG2 cells using the RNeasy mini kit (Qiagen, Valencia, CA) was subjected to cDNA synthesis using the SuperScript III first strand synthesis kit (Invitrogen, Carlsbad, CA). The resulting cDNAs were subjected to polymerase chain reaction (PCR) using primers specific for FABP3, FABP5, FABP7, or β-actin. The following primers were used: for FABP3, forward 5′-CATCGAGAAGAACGGGGATA-3′ and reverse 5′-TGCCATGAGTGAGAGTCAGG-3′; FABP5 forward 5′-CAAAACCGAGAGCACAGTGA-3′ and reverse 5′-CACGATCATCTTCCCATCCT-3′; FABP7 forward 5′-AGTGGGAAACGTGACCAAAC-3′ and 5′-TTTCTTTGCCATCCCACTTC-3′; and β-actin forward 5′-AGATGACCCAGATCATGTTTGA-3′ and reverse 5′-CACAGCTTCTCCTTAATGTCA-3′. The following cycling conditions were used: denaturation at 94 °C for 30 seconds, annealing at 58 °C for 30 seconds, and extension at 72 °C for 30 seconds for a total of 30 cycles. The resulting products were visualized on an agarose gel.

Statistical Analyses. Results are expressed as means ± SEM. Statistical significance was evaluated using two tailed unpaired *t* tests against vector-transfected or vehicle-treated controls.

ACKNOWLEDGMENTS. We thank Guo-Wei Tian for help with confocal microscopy and Adam Leonard at Bristol-Myers Squibb for helpful discussions. We also acknowledge the National Institute on Drug Abuse for support (DA9374 and DA16419).

1. Devane WA, Hanus L, Breuer A, Pertwee RG, Stevenson LA, et al. (1992) Isolation and structure of a brain constituent that binds to the cannabinoid receptor. *Science* 258:1946–1949.
2. Ahn K, McKinney MK, Cravatt BF (2008) Enzymatic pathways that regulate endocannabinoid signaling in the nervous system. *Chem Rev* 108:1687–1707.
3. Munro S, Thomas KL, Abu-Shaar M (1993) Molecular characterization of a peripheral receptor for cannabinoids. *Nature* 365:61–65.
4. Matsuda LA, Lolait SJ, Brownstein MJ, Young AC, Bonner TI (1990) Structure of a cannabinoid receptor and functional expression of the cloned cDNA. *Nature* 346:561–564.
5. de Lago E, Fernandez-Ruiz J, Ortega-Gutierrez S, Viso A, Lopez-Rodriguez ML, et al. (2002) UCM707, a potent and selective inhibitor of endocannabinoid uptake, potentiates hypokinetic and antinociceptive effects of anandamide. *Eur J Pharmacol* 449:99–103.
6. Devane WA, Dysarz FA 3rd, Johnson MR, Melvin LS, Howlett AC (1988) Determination and characterization of a cannabinoid receptor in rat brain. *Mol Pharmacol* 34:605–613.
7. Zygmunt PM, Petersson J, Andersson DA, Chuang H, Sorgard M, et al. (1999) Vanilloid receptors on sensory nerves mediate the vasodilator action of anandamide. *Nature* 400:452–457.
8. Howlett AC, Barth F, Bonner TI, Cabral G, Casellas P, et al. (2002) International Union of Pharmacology. XXVII. Classification of cannabinoid receptors. *Pharmacol Rev* 54:161–202.
9. Lambert DM, Fowler CJ (2005) The endocannabinoid system: Drug targets, lead compounds, and potential therapeutic applications. *J Med Chem* 48:5059–5087.
10. Bojesen IN, Hansen HS (2005) Membrane transport of anandamide through resealed human red blood cell membranes. *J Lipid Res* 46:1652–1659.
11. Glaser ST, Abumrad NA, Fatade F, Kaczocha M, Studholme KM, et al. (2003) Evidence against the presence of an anandamide transporter. *Proc Natl Acad Sci USA* 100:4269–4274.
12. Kaczocha M, Hermann A, Glaser ST, Bojesen IN, Deutsch DG (2006) Anandamide uptake is consistent with rate-limited diffusion and is regulated by the degree of its hydrolysis by fatty acid amide hydrolase. *J Biol Chem* 281:9066–9075.
13. Fasia L, Karava V, Siafaka-Kapadai A (2003) Uptake and metabolism of [3H]anandamide by rabbit platelets. Lack of transporter? *Eur J Biochem* 270:3498–3506.
14. Ortega-Gutierrez S, Hawkins EG, Viso A, Lopez-Rodriguez ML, Cravatt BF (2004) Comparison of anandamide transport in FAAH wild-type and knockout neurons: Evidence for contributions by both FAAH and the CB1 receptor to anandamide uptake. *Biochemistry* 43:8184–8190.
15. Sandberg A, Fowler CJ (2005) Measurement of saturable and non-saturable components of anandamide uptake into P19 embryonic carcinoma cells in the presence of fatty acid-free bovine serum albumin. *Chem Phys Lipids* 134:131–139.
16. Di Marzo V, Fontana A, Cadas H, Schinelli S, Cimino G, et al. (1994) Formation and inactivation of endogenous cannabinoid anandamide in central neurons. *Nature* 372:686–691.
17. Beltramo M, Stella N, Calignano A, Lin SY, Makriyannis A, et al. (1997) Functional role of high-affinity anandamide transport, as revealed by selective inhibition. *Science* 277:1094–1097.
18. Hillard CJ, Edgemond WS, Jarrahian A, Campbell WB (1997) Accumulation of N-arachidonoylethanolamine (anandamide) into cerebellar granule cells occurs via facilitated diffusion. *J Neurochem* 69:631–638.
19. McFarland MJ, Porter AC, Rakhshan FR, Rawat DS, Gibbs RA, et al. (2004) A role for caveolae/lipid rafts in the uptake and recycling of the endogenous cannabinoid anandamide. *J Biol Chem* 279:41991–41997.
20. Bari M, Battista N, Fezza F, Finazzi-Agro A, Maccarrone M (2005) Lipid rafts control signaling of type-1 cannabinoid receptors in neuronal cells. Implications for anandamide-induced apoptosis. *J Biol Chem* 280:12212–12220.
21. Deutsch DG, Chin SA (1993) Enzymatic synthesis and degradation of anandamide, a cannabinoid receptor agonist. *Biochem Pharmacol* 46:791–796.
22. Cravatt BF, Giang DK, Mayfield SP, Boger DL, Lerner RA, et al. (1996) Molecular characterization of an enzyme that degrades neuromodulatory fatty-acid amides. *Nature* 384:83–87.
23. Hillard CJ, Jarrahian A (2003) Cellular accumulation of anandamide: Consensus and controversy. *Br J Pharmacol* 140:802–808.
24. Glaser ST, Kaczocha M, Deutsch DG (2005) Anandamide transport: A critical review. *Life Sci* 77:1584–1604.
25. Hillard CJ, Jarrahian A (2000) The movement of N-arachidonoylethanolamine (anandamide) across cellular membranes. *Chem Phys Lipids* 108:123–134.
26. Furuhashi M, Hotamisligil GS (2008) Fatty acid-binding proteins: Role in metabolic diseases and potential as drug targets. *Nat Rev Drug Discov* 7:489–503.
27. Owada Y, Yoshimoto T, Kondo H (1996) Spatio-temporally differential expression of genes for three members of fatty acid binding proteins in developing and mature rat brains. *J Chem Neuroanat* 12:113–122.
28. Owada Y, Suzuki I, Noda T, Kondo H (2002) Analysis on the phenotype of E-FABP-gene knockout mice. *Mol Cell Biochem* 239:83–86.
29. Owada Y, Suzuki R, Iwasa H, Spener F, Kondo H (2002) Localization of epidermal-type fatty acid binding protein in the thymic epithelial cells of mice. *Histochem Cell Biol* 117:55–60.
30. Murphy EJ, Barcelo-Coblijn G, Binas B, Glatz JF (2004) Heart fatty acid uptake is decreased in heart fatty acid-binding protein gene-ablated mice. *J Biol Chem* 279:34481–34488.
31. Pelsers MM, Hanhoff T, Van der Voort D, Arts B, Peters M, et al. (2004) Brain- and heart-type fatty acid-binding proteins in the brain: tissue distribution and clinical utility. *Clin Chem* 50:1568–1575.
32. Furuhashi M, Tuncman G, Gorgun CZ, Makowski L, Atsumi G, et al. (2007) Treatment of diabetes and atherosclerosis by inhibiting fatty-acid-binding protein aP2. *Nature* 447:959–965.
33. Schug TT, Berry DC, Shaw NS, Travis SN, Noy N (2007) Opposing effects of retinoic acid on cell growth result from alternate activation of two different nuclear receptors. *Cell* 129:723–733.
34. Wei BQ, Mikkelsen TS, McKinney MK, Lander ES, Cravatt BF (2006) A second fatty acid amide hydrolase with variable distribution among placental mammals. *J Biol Chem* 281:36569–36578.
35. Patricelli MP, Lashuel HA, Giang DK, Kelly JW, Cravatt BF (1998) Comparative characterization of a wild type and transmembrane domain-deleted fatty acid amide hydrolase: Identification of the transmembrane domain as a site for oligomerization. *Biochemistry* 37:15177–15187.
36. Kanaji S, Iwahashi J, Kida Y, Sakaguchi M, Mihara K (2000) Characterization of the signal that directs Tom20 to the mitochondrial outer membrane. *J Cell Biol* 151:277–288.
37. Barr FA, Puype M, Vandekerckhove J, Warren G (1997) GRASP65, a protein involved in the stacking of Golgi cisternae. *Cell* 91:253–262.
38. Oddi S, Bari M, Battista N, Barsacchi D, Cozzani I, et al. (2005) Confocal microscopy and biochemical analysis reveal spatial and functional separation between anandamide uptake and hydrolysis in human keratinocytes. *Cell Mol Life Sci* 62:386–395.
39. Day TA, Rakhshan F, Deutsch DG, Barker EL (2001) Role of fatty acid amide hydrolase in the transport of the endogenous cannabinoid anandamide. *Mol Pharmacol* 59:1369–1375.
40. Deutsch DG, Glaser ST, Howell JM, Kunz JS, Puffenbarger RA, et al. (2001) The cellular uptake of anandamide is coupled to its breakdown by fatty-acid amide hydrolase. *J Biol Chem* 276:6967–6973.
41. Fezza F, Oddi S, Di Tommaso M, De Simone C, Rapino C, et al. (2008) Characterization of biotin-anandamide, a novel tool for the visualization of anandamide accumulation. *J Lipid Res* 49:1216–1223.
42. Howlett AC (1985) Cannabinoid inhibition of adenylate cyclase. Biochemistry of the response in neuroblastoma cell membranes. *Mol Pharmacol* 27:429–436.
43. Maurelli S, Bisogno T, De Petrocellis L, Di Luccia A, Marino G, et al. (1995) Two novel classes of neuroactive fatty acid amides are substrates for mouse neuroblastoma 'anandamide amidohydrolase'. *FEBS Lett* 377:82–86.
44. Murphy EJ, Owada Y, Kitanaka N, Kondo H, Glatz JF (2005) Brain arachidonic acid incorporation is decreased in heart fatty acid binding protein gene-ablated mice. *Biochemistry* 44:6350–6360.
45. Owada Y, Abdelwahab SA, Kitanaka N, Sakagami H, Takano H, et al. (2006) Altered emotional behavioral responses in mice lacking brain-type fatty acid-binding protein gene. *Eur J Neurosci* 24:175–187.
46. Kurtz A, Zimmer A, Schnutgen F, Bruning G, Spener F, et al. (1994) The expression pattern of a novel gene encoding brain-fatty acid binding protein correlates with neuronal and glial cell development. *Development* 120:2637–2649.
47. Hanhoff T, Lucke C, Spener F (2002) Insights into binding of fatty acids by fatty acid binding proteins. *Mol Cell Biochem* 239:45–54.
48. Sulsky R, Magnin DR, Huang Y, Simpkins L, Taunk P, et al. (2007) Potent and selective biphenyl azole inhibitors of adipocyte fatty acid binding protein (aFABP). *Bioorg Med Chem Lett* 17:3511–3515.
49. Patricelli MP, Cravatt BF (2001) Proteins regulating the biosynthesis and inactivation of neuromodulatory fatty acid amides. *Vitam Horm* 62:95–131.
50. Stremmel W, Pohl L, Ring A, Herrmann T (2001) A new concept of cellular uptake and intracellular trafficking of long-chain fatty acids. *Lipids* 36:981–989.
51. Feng L, Hatten ME, Heintz N (1994) Brain lipid-binding protein (BLBP): A novel signaling system in the developing mammalian CNS. *Neuron* 12:895–908.
52. Maccarrone M, Fiorucci L, Erba F, Bari M, Finazzi-Agro A, et al. (2000) Human mast cells take up and hydrolyze anandamide under the control of 5-lipoxygenase and do not express cannabinoid receptors. *FEBS Lett* 468:176–180.
53. Sun YX, Tsuboi K, Zhao LY, Okamoto Y, Lambert DM, et al. (2005) Involvement of N-acylethanolamine-hydrolyzing acid amidase in the degradation of anandamide and other N-acylethanolamines in macrophages. *Biochim Biophys Acta* 1736:211–220.
54. Luxon BA, Weisiger RA (1993) Sex differences in intracellular fatty acid transport: role of cytoplasmic binding proteins. *Am J Physiol* 265:G831–G841.
55. Weisiger RA (2007) Mechanisms of intracellular fatty acid transport: Role of cytoplasmic-binding proteins. *J Mol Neurosci* 33:42–44.
56. Sun Y, Alexander SPH, Kendall DA, Bennett AJ (2008) *Involvement of fatty acid binding proteins in the transport of endocannabinoids to peroxisome proliferator activated receptors* (International Cannabinoid Research Society, Burlington, VT), p 17. 1.
57. Rakhshan F, Day TA, Blakely RD, Barker EL (2000) Carrier-mediated uptake of the endogenous cannabinoid anandamide in RBL-2H3 cells. *J Pharmacol Exp Ther* 292:960–967.
58. Alexander JP, Cravatt BF (2006) The putative endocannabinoid transport blocker LY2183240 is a potent inhibitor of FAAH and several other brain serine hydrolases. *J Am Chem Soc* 128:9699–9704.
59. Dickason-Chesterfield AK, Kidd SR, Moore SA, Schaus JM, Liu B, et al. (2006) Pharmacological characterization of endocannabinoid transport and fatty acid amide hydrolase inhibitors. *Cell Mol Neurobiol* 26:407–423.
60. Ortar G, Ligresti A, De Petrocellis L, Morera E, Di Marzo V (2003) Novel selective and metabolically stable inhibitors of anandamide cellular uptake. *Biochem Pharmacol* 65:1473–1481.
61. Fegley D, Kathuria S, Mercier R, Li C, Goutopoulos A, et al. (2004) Anandamide transport is independent of fatty-acid amide hydrolase activity and is blocked by the hydrolysis-resistant inhibitor AM1172. *Proc Natl Acad Sci USA* 101:8756–8761.
62. Fu J, Gaetani S, Oveisi F, Lo Verme J, Serrano A, et al. (2003) Oleylethanolamide regulates feeding and body weight through activation of the nuclear receptor PPAR-alpha. *Nature* 425:90–93.
63. Lo Verme J, Fu J, Astarita G, La Rana G, Russo R, et al. (2005) The nuclear receptor peroxisome proliferator-activated receptor-alpha mediates the anti-inflammatory actions of palmitoylethanolamide. *Mol Pharmacol* 67:15–19.
64. Koutek B, Prestwich GD, Howlett AC, Chin SA, Salehani D, et al. (1994) Inhibitors of arachidonoyl ethanolamide hydrolysis. *J Biol Chem* 269:22937–22940.
65. McKinney MK, Cravatt BF (2005) Structure and function of fatty acid amide hydrolase. *Annu Rev Biochem* 74:411–432.
66. Di Marzo V (2008) Targeting the endocannabinoid system: to enhance or reduce? *Nat Rev Drug Discov* 7:438–455.